Advanced imaging determinants of intracranial aneurysm growth and rupture

Katwijk-Leemans, E.L.

Publication date
2020
Document Version
Other version
License
Other

5

CHAPTER 5.

Intracranial aneurysm growth: consistency of morphological changes

Leemans E.L., Cornelissen B.M.W., Said M., van den Berg R., Slump C.H., Marquering H.A., Majoie C.B.L.M. Intracranial aneurysm growth: Consistency of morphological changes. Neurosurgical Focus, 2019 47 (1), art. no. E5

DOI: 10.3171/2019.4.focus1987

Abstract

Background:

Previous studies showed a relation between growth and rupture of intracranial aneurysms. Additionally, several morphological characteristics are frequently measured to estimate rupture risk. Little is known about how the rupture risk is associated with morphological characteristics change during growth.

Methods:

We have retrospectively identified patients with longitudinal MRA-imaging of unruptured growing aneurysms. The MRA images had an in-plane resolution of 0.2-0.5 mm and a slice thickness of 0.2-0.75 mm. Therefore, growth was defined as an increase of at least 0.5 mm in 2 directions or 1 mm in 1 direction. Based on MRA-images, we semi-automatically segmented the aneurysm and the peri-aneurysmal vasculature. We measured twelve morphological characteristics automatically. These characteristics were related to size (diameter, height, width, neck diameter, volume, surface area, aspects ratio, height-width ratio and bottleneck factor) and shape (ellipticity index, non-sphericity index and undulation index) of the aneurysm. Morphological characteristics before and after growth were compared using the Wilcoxon Singed rank test.

Results:

We included 31 patients with 38 growing aneurysms. The aneurysms growth was detected after 218 weeks (range: 23-567 weeks). A significant increase was seen in all size related characteristics, the bottleneck factor also significantly increased (from 1.00, IQR: 0.85-1.04 to 1.03, IQR: 0.93-1.18), while the ellipticity index decreased (from 0.26, IQR: 0.25-0.28 to 0.25, IQR: 0.24-0.26). The change in size ratios and shape indices varied largely between patients. Larger aneurysm more often showed an increase in shape ratios.

Conclusions:

Although growth, the size related characteristics, the bottle neck factor and the ellipticity index change significantly during growth, most size ratios and shape indices show inconsistent changes between aneurysms. This suggests that, for an accurate rupture prediction, morphological parameters need to be re-assessed after growth.

Introduction

An increasing number of unruptured aneurysms is being detected due to improvements in, and the wide availability and use of imaging.[14] Only a small number of intracranial aneurysms will eventually rupture. Rupture often leads to death or severe disability and poses a considerable clinical and socio-economic burden.[17] As aneurysm treatment also poses considerable risks[22,25], the risk of rupture must outweigh treatment risk. Current guidelines recommend to take the following factors into account when deciding upon treatment: size, irregularity, location, aneurysm growth, family history for subarachnoid hemorrhage, age, hypertension[23,35], previous subarachnoid hemorrhage, and the presence of comorbidities.[7,16,23,33,35]

If an aneurysm is left untreated, guidelines recommend performing periodic follow-up imaging of the aneurysm. It has been reported that approximately 10% of the aneurysms show growth on follow-up imaging.[11] Aneurysmal growth is associated with an increasing risk of rupture, as growing aneurysms have proven to be unstable.[35] Growth patterns differ, for instance some grow globally while others form a bleb. Different growth patterns might have a different rupture risk as different pathological processes underlie the growth.[27] Thus, more understanding of aneurysm growth is needed to improve the management of unruptured aneurysms.

Next to size, several other aneurysmal morphological characteristics, such as aspects ratio (AR) and ellipticity index (EI), are frequently used to predict which aneurysms are can be expected to rupture.[10,12,18,20,21,27] Each available index describes a different aspect of the aneurysms morphology. These characteristics may change as aneurysms grow. The dynamics of these characteristics during aneurysms growth is still unclear. Nonetheless, these characteristics are used to predict the risk of rupture at a given moment in time. The aim of this study is to provide insights into how morphological characteristics, associated with rupture, change during aneurysms growth.

Methods

Population

We retrospectively included all patients with a saccular unruptured intracranial aneurysm and longitudinal imaging from 2012 to 2016 at our tertiary care referral center. In this population of 253 patients with 333 aneurysms, 55 aneurysms were marked as growing aneurysms based on the imaging report by the neuroradiologist. These reports reported a change in size of more than 1 millimeter in one direction, 0.5 millimeter in two directions, or did not show a significant change in shape.[4] We performed longitudinal imaging with either CTA or MRA. The MRA consisted of (3D) time of flight or contrast enhanced MRA. We excluded all patients with only CTA imaging available (n = 9), as most CTA images contained slices of > 0.75mm and thus no accurate segmentation could be made. Additionally, we excluded 11 scans because of poor imaging quality (n = 2), different MRA sequences (n = 1), no available time of flight imaging (n = 4) and imaging after treatment (n = 2). As a result, this study included 31 patients with 38 growing aneurysms. All included MRA images were made on a scanner of Philips medical systems. The scan parameters were: TR: 20-47 ms, TE: 1.5-6.4 ms, in plane resolution: 0.2-0.5 mm, slice thickness: 0.2-0.75mm. The institution's review board waived the requirement for informed consent because no diagnostics other than routine clinical imaging were used in this study.

Morphology

To assess aneurysm morphology, we used the following longitudinal images: baseline imaging, all imaging showing growth, and final image of the untreated aneurysm. As a result, for each patient the aneurysm morphology was determined at 2 to 4 moments in time. We focused the analysis on the imaging at baseline and the final available imaging. The other moments in time were used to evaluate when growth was first detected and whether an aneurysm continued to grow after initial detection.

We have segmented the aneurysm and peri-aneurysmal vasculature on the available imaging using the Vascular Modeling Toolkit[2] Both thresholding and a Sato vesselness filter were used for the automated segmentation. Each model was visually inspected by an expert with more than 2 years' experience in neurovascular imaging (EL). If needed, the segmentations were manually corrected to reduce inaccuracies due to imaging artefacts such as flow dispersion, saturation, and partial voluming. The manual corrections were performed with ITK-snap 3.6.0.

In four aneurysms (11 models), it was difficult to differentiate the aneurysm from its surrounding vessels; therefore, these models were also corrected by an experienced neuroradiologist (CM). Subsequently, the surfaces of the resulted segmentations were smoothed with the build in Taubin-smoothing algorithm of the Vascular Modeling Toolkit, hereby removing high-frequency artefacts without shrinking of the surface.[32] The following smoothing parameters were used: passband factor of 0.05, and 20 iterations.

To calculate the aneurysms morphological characteristics, the aneurysm volume and neck plane were automatically determined. First, the algorithm reconstructed the original parent vessel. We used the parent vessel reconstruction algorithm by Ford et al.[13] This parent vessel reconstruction consists of creating multiple centerlines in the parent vessel; determining where the aneurysms deviates from the parent vessel and reconstructing the original vessel using the Voronoi diagram (see Figure 5.1A-F). With the delineation of the parent artery, the aneurysm surface was extracted (Figure 5.1). The aneurysms surface is here defined as the part of the total surface that not coincides the parent vessel surface.

In current clinical practice, several morphological characteristics are measured after defining the aneurysm neck-plane. The neck plane is detected using the methodology reported by Piccinelli et al.[26] By defining planes at multiple orientations on the centerline the optimal neck-plane can be found (Figure 5.1G), which is the plane with the smallest area and which is the closed to, but not intersecting, the parent vessel.

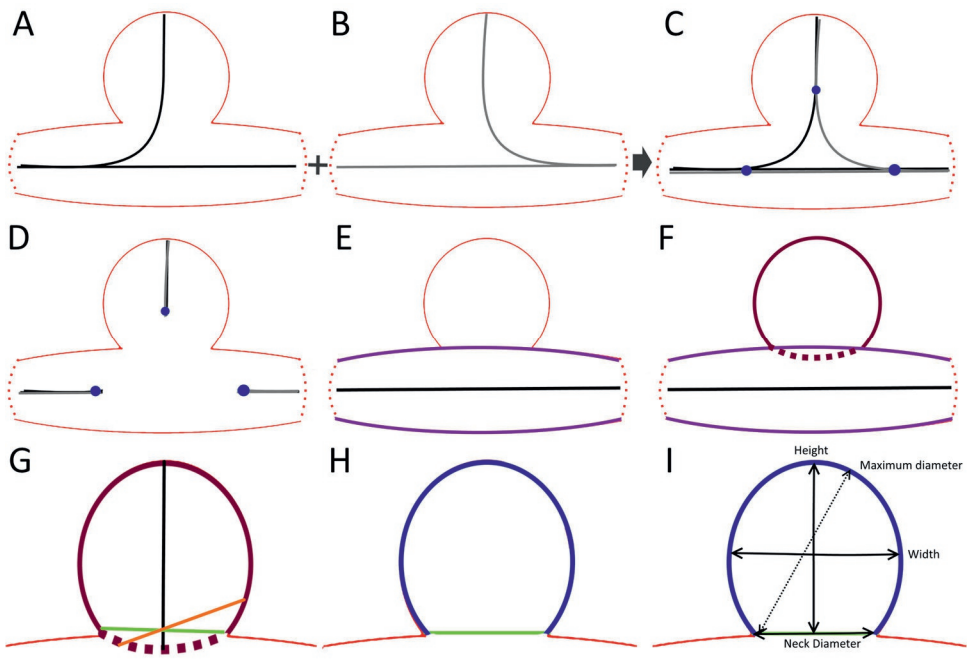

Figure 5.1. Parent vessel reconstruction and aneurysm assessment. A. Forward centerline. B. Backward centerline. C. Combination of centerline and identification of the clipping points (blue). D. Clipping at the clipping points. E. Reconstruction of the parent vessel and therefore cannot be a neck plane, the green plane does not intersect and is marked as a possible neck plane. H. Selection of the perfect neck plane (green) and extraction of the aneurysm surface from the neck onwards. I. Evaluating aneurysm morphology.

Morphological characteristics

With the delineation of the aneurysm surface and the neck-plane, the morphological characteristics were automatically calculated. The characteristics can be divided into four groups: 2D size characteristics, size ratios, 3D size characteristics and shape characteristics. Additional to the shape characteristics, an experienced neuroradiologist assessed the irregularity at baseline. All characteristics were measured in accordance with the definitions of Raghavan et al.[27]

The 2D size characteristics consist of the maximum diameter, height, width. These were measures as depicted in Figure 5.1F. The maximum diameter is the maximum distance found between two points on the aneurysms surface. The aneurysm height is defined as the longest distance from the center of the neck-plane to the

aneurysm dome. The aneurysm width depicts the longest distance perpendicular to the measurement of the aneurysm height. In addition to the 2D size characteristics, two 3D size characteristics are determined, the aneurysm volume and surface area (SA).

With these 2D size characteristics, several size ratios are determined; height-width ratio (HWR), bottleneck factor (BNF), aspect ratio (AR). The height-width ratio depicts the difference between the height and the width of the aneurysm. The bottleneck factor is the ratio between the width and aneurysms neck diameter, it therefore shows if an aneurysm has a small or a broad base. The aspect ratio is the ratio between the height and the neck diameter; it thus shows how elongated the aneurysm is.

The last characteristics are the shape characteristics; ellipticity index (EI), non-sphericity index (NSI), and undulation index (UI). For these indices, the convex hull is determined. The convex hull of an aneurysm is the smallest convex volume that encloses the aneurysm volume. The ellipticity index characterizes the deviation of the aneurysm convex hull (as described by the convex hull volume (V_{ch}) and surface area (SA_{ch})) from a perfect sphere ($EI = 1 - 18\pi^{1/3}\frac{V_{ch}^{2/3}}{SA_{ch}}$). The NSI is similar to the EI but instead of the convex hull volume and surface area, the volume and surface area of the aneurysm are used. It is therefore influenced by both ellipticity and surface irregularities (undulations). The UI captures the aneurysm irregularity, as it compares the aneurysm volume with the volume of the convex hull ($UI = 1 - \frac{V}{V_{ch}}$, a completely regular aneurysm without any undulations will have an UI of 0.

Statistics

We tested all variables for normality using a Shapiro-Wilk test. Normally distributed values were reported as mean ± standard deviation; non-normally distributed values were reported as median and interquartile range (IQR 25-75%). Morphological characteristics at baseline were compared with the characteristics at the final imaging using a paired T-test for normally distributed variables and a Wilcoxon Singed rank test for non-normal distributed variables. A P-value below 0.05 was considered statistically significant.

Results

We included 31 patients with 38 growing aneurysms with in total 118 MR-imaging studies. Figure 5.2 shows two examples. The clinical characteristics can be found in Table 1. Most patients had multiple aneurysms (n = 21, 68%) and were female (n = 26, 84%). In about a third of the cases, the patient had a previous subarachnoid hemorrhage (n = 9, 29%) of another aneurysm.

Table 1. Clinical characteristics

Characteristic	Mean ± SD or n (%)
Sex (female)	27 (82%)
Aneurysm multiplicity	21 (68%)
Age at baseline (years)	51 ± 11
Previous subarachnoid hemorrhage	9 (29%)
Location of the growing aneurysm	
Internal carotid artery (ICA)	8 (21%)
Anterior cerebral artery (ACA) / Anterior communicating artery (AcomA)	8 (21%)
Middle cerebral artery (MCA)	16 (42%)
Posterior communicating artery (PcomA) / Posterior circulation	6 (16%)
Aneurysm shape at baseline (regular)	32 (84%)

Aneurysm growth was detected after 218 weeks (range: 23-567 weeks). Twelve of the growing aneurysms (32%) were treated and one (3%) ruptured during follow-up. The aneurysms were treated between 12 and 283 weeks after the detection of growth (4 within 6 months from the detection of growth). The aneurysm ruptured 28 weeks after the detection of growth. Blebs were formed in two aneurysms (5%), while eight (21%) aneurysms had a clear change in shape (i.e. new multiple lobulations or wall protrusions). On average, the aneurysms grew 1.8 ± 2.1 mm; no differences were seen between aneurysm locations. In 11 (29%) cases, growth was detected on multiple scans after the baseline imaging, but for 13 (34%) cases, we only have two sets of images and thus for these cases it could not be determined if these cases were still unstable after growth.

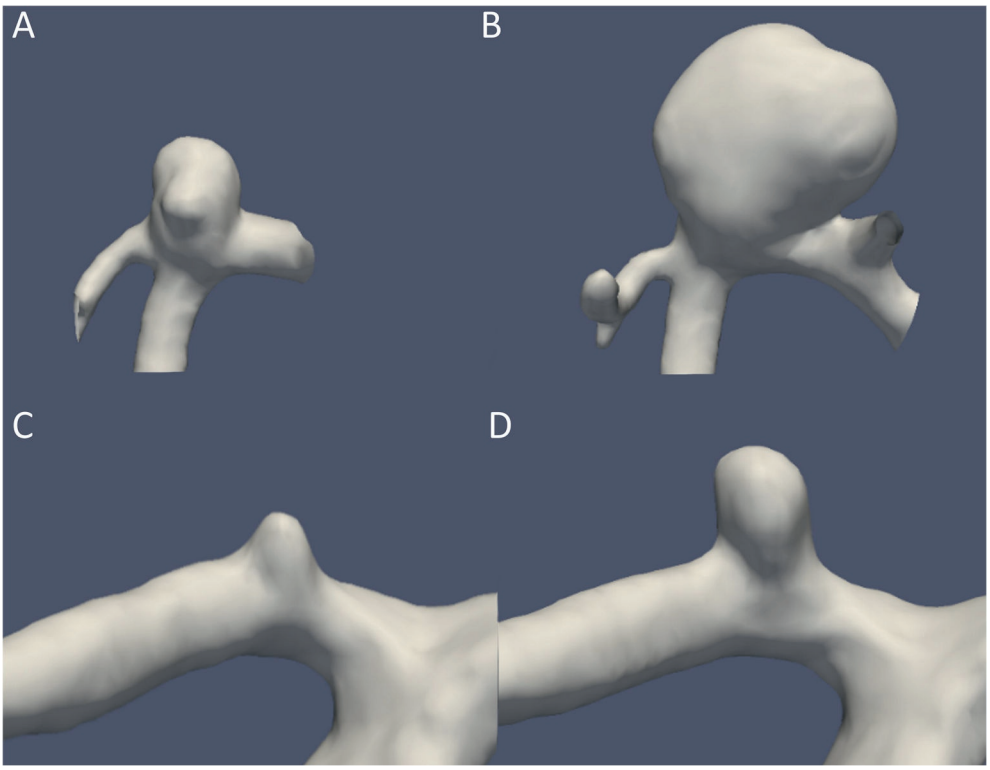

Figure 5.2. Examples of aneurysms before (A, C) and after growth (B, D). The aneurysm in A and B also shows a clear change in shape.

Morphological characteristics:

Nine out of the twelve morphological characteristics changed significantly after growth, see Table 2. Most of these characteristics are associated with the aneurysm size. A significant increase was seen in diameter, width, height, neck diameter, BNF, volume, and surface area, while the EI and UI decreased. On average, the aneurysm width increased more than the aneurysm height, but the change in height-width ratio was insignificant. The increase in BNF indicates that during growth the aneurysm neck grows slower or less than the aneurysm width. The decrease in ellipticity index indicates that the aneurysm convex hull deviates more from a perfect sphere and thus that the aneurysm becomes less spherical or has more undulations.

Table 2. Morphological characteristics at baseline and final imaging

Characteristic	Baseline Median (IQR)	Final Median (IQR)	Difference Mean (SD)	p
Diameter (mm)	5.0 (3.4, 7.0)	6.9 (4.9, 9.0)	1.8 (2.1)	0.01
Width (mm)	3.6 (2.6, 5.5)	5.04 (3.9, 7.9)	1.6 (1.7)	0.003
Height (mm)	2.2 (1.5, 3.9)	3.3 (2.1, 5.2)	1.0 (1.6)	0.02
Neck Diameter (mm)	3.6 (2.5, 5.5)	4.58 (3.2, 6.9)	1.2 (1.2)	0.01
Bottleneck Factor	1.00 (0.85, 1.04)	1.03 (0.93, 1.18)	0.09 (0.35)	0.05
Aspect Ratio	0.63 (0.50, 0.77)	0.68 (0.57, 0.87)	0.06 (0.20)	0.06
Height-Width Ratio	0.63 (0.54, 0.78)	0.68 (0.49, 0.81)	0.01 (0.3)	0.60
Volume (mm^3)	13.9 (5.0, 51.3)	44.0 (13.4, 105.7)	41.7 (66.8)	0.01
Surface Area (mm^2)	31.9 (16.8, 74.7)	71.8 (29.5, 120.5)	36.4 (46.6)	0.01
Ellipticity index	0.26 (0.25, 0.28)	0.25 (0.24, 0.26)	-0.01 (0.02)	0.02
Non-sphericity index	0.19 (0.17, 0.22)	0.19 (0.17, 0.22)	0.00 (0.04)	0.82
Undulation index	0.23 (0.14, 0.35)	0.18 (0.13, 0.22)	-0.05 (0.11)	0.02

As can be seen in Figure 5.3, the 2D and 3D size related characteristics increase in most patients during growth. However, the change in width is more consistent with the aneurysm diameter than the change in height. No clear trends were seen for the size ratios (AR, BNF, and HWR); in some aneurysms, these ratios increase but in other aneurysms, these ratios decrease. In most aneurysms, the EI decreased during growth. However, some aneurysms show a stable or increase in EI. The UI follows a similar trend.

Figure 5.4 shows for each morphological characteristic the relation of the magnitude of the measured change with the baseline diameter. No dependencies on baseline diameter were seen for the 2D size characteristics and the size indices. The aneurysm volume and surface area show larger changes with an increasing baseline diameter. Additionally, the shape indices seem to decrease with smaller baseline diameters but increase with larger diameters.

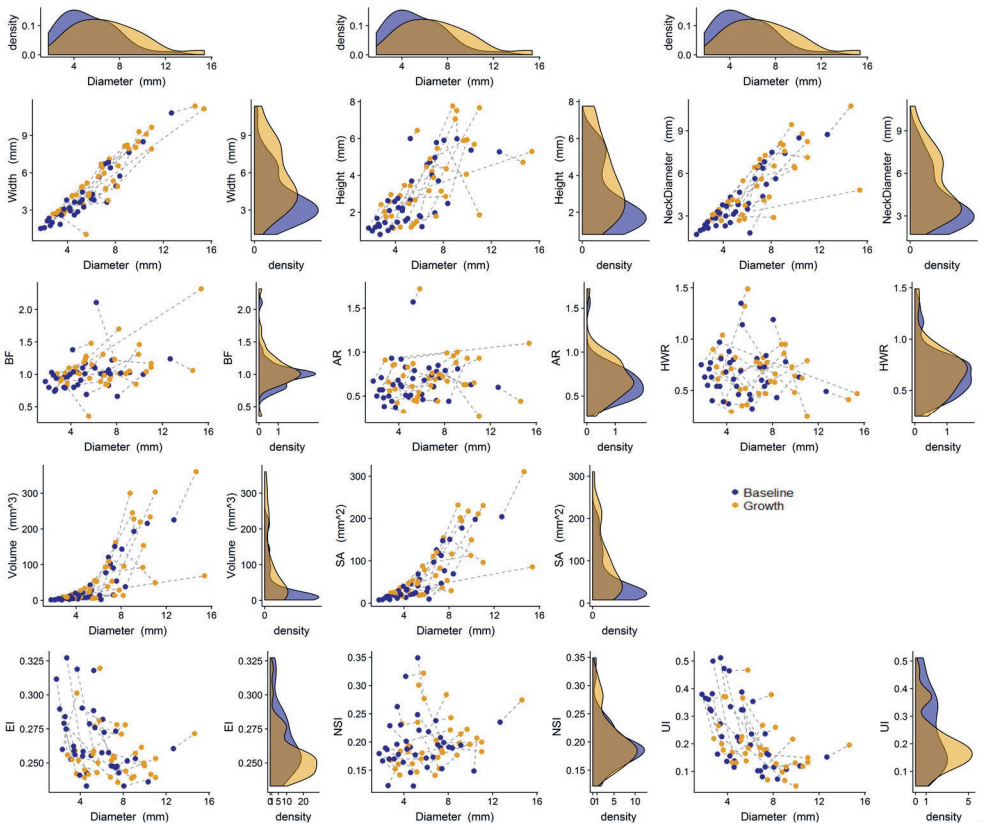

Figure 5.3. Scatter and density plots for each morphological characteristic versus diameter. The density plots of the diameter are displayed on the first row. The density plots of each characteristic are displayed vertically (column 2, 4, and 6). Blue dots and density plots represent the baseline values, orange dots and plots the values after growth (at the time of the final imaging). The dotted lines connect the baseline and final value of one aneurysm.

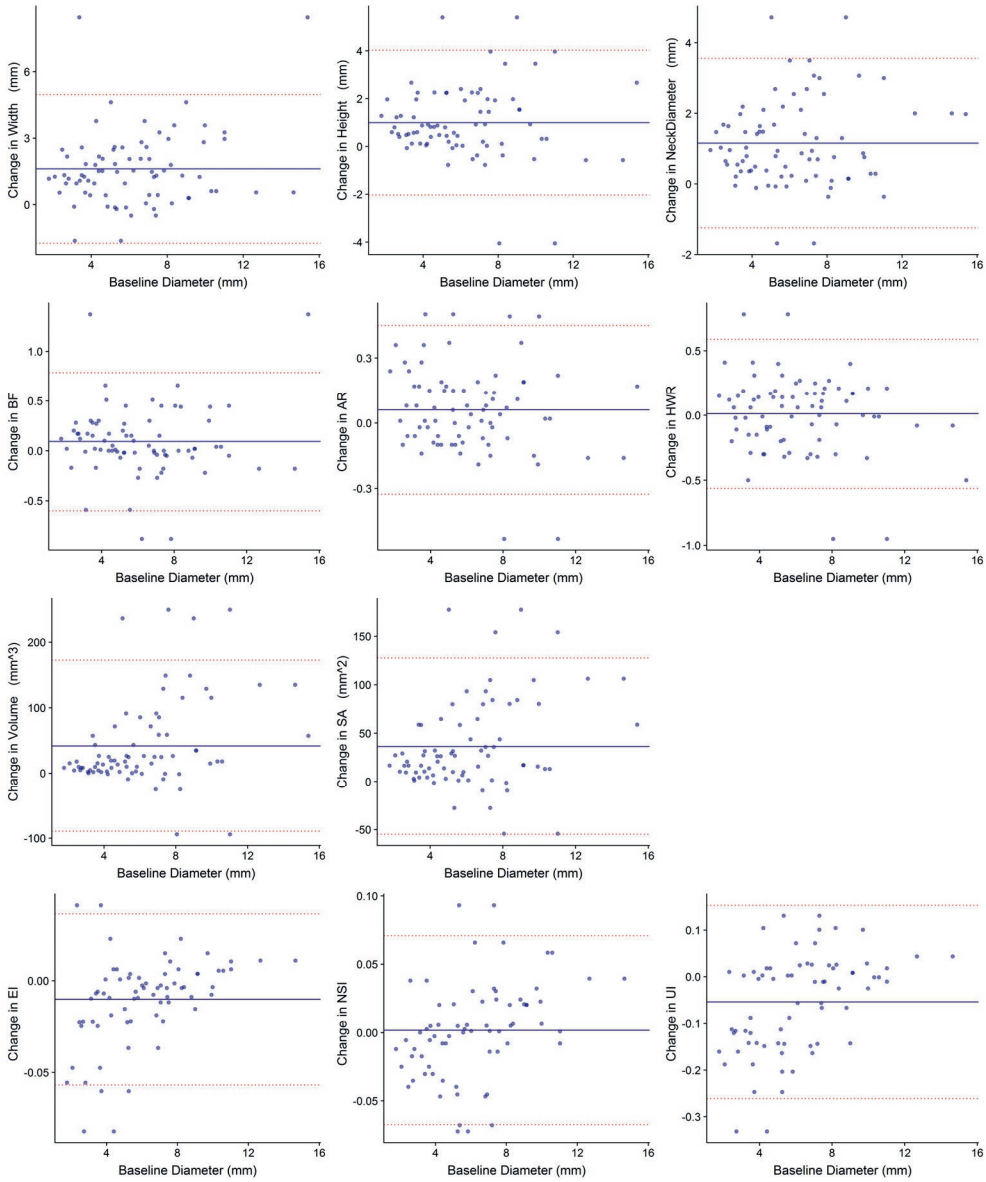

Figure 5.4. Modified Bland-Altman plots showing the change in the morphological characteristics versus the baseline diameter. Blue line shows the average change, the dotted red lines show the upper and lower border of the 95% confidence interval.

Discussion

This study evaluated to which extent commonly measured morphological characteristics change during aneurysm growth. A significant increase was seen in the 2D and 3D size related characteristics and the bottleneck factor (BNF) during growth of intracranial aneurysms. The ellipticity index (EI) and undulation index (UI) significantly decreased. Both the size ratios and shape indices show inconsistent trends, in some aneurysms these ratios increased but in other aneurysms the values decreased. Based on the Bland-Altman plots, the shape indices seem to decrease with smaller baseline diameters but increase with larger diameters.

The aneurysm growth rate of our population (19%) is in line with other studies that reported growth rates between 4 and 45%.[5] Several studies showed that aneurysms size and irregularity is a strong predictor for growth.[3] Our study showed that the change in most parameters was not dependent on the size at baseline, but a larger aneurysm diameter at baseline often resulted in an increase instead of decrease in the shape indices (EI, NSI, and UI). Indicating that larger aneurysms are more likely to become irregular or form a bleb during growth while smaller aneurysm often become more regular and spherical. As aneurysm irregularity is related to both growth[4] and rupture[19,21], the rupture risk of these smaller aneurysms might decrease during growth. It is yet unknown whether the other presented rupture risk related characteristics predict growth. Nevertheless, our study provides insights into what happens to these characteristics during growth.

Previous studies reported higher aspect ratio[10,12,27,38], BNF[12], height-width ratio[12], UI[10,27,37], and NSI[10,27,37] and a lower EI[10,27,37] in ruptured aneurysms. Growing aneurysms have proven to be unstable and more prone to rupture.[35] Therefore, one might expect that after growth aneurysms have a morphology similar to the ruptured aneurysms of previous studies. Our study only showed a significant increase for the BNF and a significant lower EI. Thus, most of these rupture related characteristics did not change significantly after growth. This might be because many studies use the imaging after rupture to determine the morphology, but it has been shown that the morphology changes after rupture.[30] Additionally, we did observe inconsistent changes in morphology between aneurysms. The difference in morphological change between these aneurysms might indicate a different rupture risk. Some aneurysms stabilize after growth. Although aneurysm growth is related to rupture, not every growing aneurysm ruptures. Further research is needed to evaluate whether the difference in growth patterns can be used to predict rupture. With morphological changes the hemodynamical environment also changes which could further influence the rupture risk.[8,9,31,34] As aneurysm

hemodynamics could influence the aneurysm wall[24], these changes might (de)stabilize the aneurysm.

Currently, the rupture risk is often estimated based at a single moment in time. Such an approach neglects the dynamic aspect of an aneurysm. Therefore, evaluating rupture risk based on a single moment in time might be unreliable. As our study shows, there is a large variability in the changes in morphology during growth. Therefore, these indices might not predict rupture at a moment point in time. Reassessing the parameters, during and after growth, likely gives more extensive information on the aneurysm stability and rupture risk.

Only a small portion of the aneurysms in our dataset was treated after growth due to the estimated low rupture risk after growth. A large portion of the aneurysms was at the MCA (42%) and the diameter after growth was often below 7mm. Although some patients had an earlier SAH from another aneurysm, the 5 year cumulative rupture risk is still small (0.4-0.9% (as estimated based on the PHASES-core)[16]). As the risk of endovascular treatment in these patients was higher (mortality 1-2% and morbidity of 4-10%[25,28]), most patients were not treated and followed with additional imaging. However, one should be aware that during growth the neck diameter often also increases, therefore an aneurysm with increased size does not automatically implicate an easier endovascular procedures.[15] When choosing for conservative treatment after growth, shorter intervals between imaging can be recommended.

A limitation of this study is that the measurements of the morphological characteristics depend on the performed segmentations.[6] The aneurysm lumen might appear smaller or incomplete on TOF-MRA due to slow flow artefacts. To optimize accuracy, all segmentations were performed on MRA imaging and were subsequently inspected by an experienced neuroradiologist. Additionally, we used the same imaging sequence at baseline and follow-up imaging, thus the increase in size was independent of the imaging method. More accurate measurements can be obtained with 3D rotational angiography (3DRA) due to the high resolution and signal to noise ratios.[1] However, follow-up imaging is rarely done with 3DRA, as this method is invasive.

The resolution (both in plane and in the slice direction) was around 0.5mm, which was our detection limit for aneurysm growth. Previous studies showed that the detection rate for aneurysm growth was high for growth above 0.4mm[36], but smaller enlargement might be missed. Nevertheless, these smaller enlargements

are also difficult to detect on other modalities and might have limited clinical relevance.

We quantified morphological shape using the EI, UI and NSI as defined by Raghavan et al.[27] By automating the quantification method the measurements are objective and repeatable, while automation preserves a close connection to the current measurement methodology. Although the used neck-plane detection method as presented by Piccinelli et al[26] has shown to be in concordance with manually positioned planes, the algorithm sometimes misplaces the neck in wide neck aneurysms and aneurysms with vessels originating from the aneurysms base. To prevent such errors, the measured characteristics were checked and in case of misplacement of the neck-plane the parent vessel and aneurysm centerline were manually adjusted. Some of the measures are based on the aneurysm neck size; it has been shown that this measure differs between imaging modalities.[29] In this study we used the same modality before and after growth hereby minimizing the differences within patients.

A selection bias is present in our study population as aneurysms with a high risk of rupture are immediately treated. This study thus only included conservative managed aneurysms. Therefore, our study population has a relatively large amount of small and MCA aneurysms. However, the results of this study provide insight in the aneurysms that are left untreated.

To conclude, we have shown that during growth the intracranial aneurysmal morphological characteristics change. This change was only significant for the size related characteristics, the bottleneck factor and ellipticity index. Most size ratios and shape indices show inconsistent changes between aneurysms during growth. This suggests that, we must re-assess morphological parameters after growth for accurate rupture prediction. Future studies should explore the inconsistencies in morphological change between aneurysms, as different growth patterns might indicate different pathologies and therefore different rupture risks.

References

1. Ajam A, Aziz AA, Asirvadam VS, Muda AS, Faye I, Safdar Gardezi SJ. A Review on Segmentation and Modeling of Cerebral Vasculature for Surgical Planning. IEEE Access. 2017;5:15222-15240. doi:10.1109/ACCESS.2017.2718590.
2. Antiga L, Piccinelli M, Botti L, Ene-Iordache B, Remuzzi A, Steinman DA. An image-based modeling framework for patient-specific computational hemodynamics. Med Biol Eng Comput. 2008;46(11):1097-1112. doi:10.1007/s11517-008-0420-1.
3. Backes D, Rinkel GJE, Greving JP, et al. ELAPSS score for prediction of risk of growth of unruptured intracranial aneurysms. Neurology. 2017;88(17):1-8. doi:10.1212/WNL.0000000000003865.
4. Backes D, Rinkel GJE, Laban KG, Algra A, Vergouwen MDI. Patient- and Aneurysm-Specific Risk Factors for Intracranial Aneurysm Growth: A Systematic Review and Meta-Analysis. Stroke. 2016;47(4):951-957. doi:10.1161/STROKEAHA.115.012162.
5. Backes D, Vergouwen MDI, Groenestege ATT, et al. PHASES Score for Prediction of Intracranial Aneurysm Growth. Stroke. 2015;46(5):1221-1227. doi:10.1161/STROKEAHA.114.008198.
6. Berg P, Voß S, Saalfeld S, et al. Multiple Aneurysms AnaTomy CHallenge 2018 (MATCH): Phase I: Segmentation. Cardiovasc Eng Technol. 2018;9(4):565-581. doi:10.1007/s13239-018-00376-0.
7. Bijlenga P, Gondar R, Schilling S, et al. PHASES Score for the Management of Intracranial Aneurysm. Stroke. 2017:STROKEAHA.117.017391. doi:10.1161/STROKEAHA.117.017391.
8. Cebral J, Ollikainen E, Chung BJ, et al. Flow Conditions in the Intracranial Aneurysm Lumen Are Associated with Inflammation and Degenerative Changes of the Aneurysm Wall. Am J Neuroradiol. 2017;38(1):119-126. doi:10.3174/ajnr.A4951.
9. Cebral JR, Raschi M. Suggested connections between risk factors of intracranial aneurysms: a review. Ann Biomed Eng. 2013;41(7):1366-1383. doi:10.1007/s10439-012-0723-0.
10. Dhar S, Tremmel M, Mocco J, et al. Morphology Parameters for Intracranial Aneurysm Rupture Risk Assessment. Neurosurgery. 2008;63(2):185-197. doi:10.1227/01.NEU.0000316847.64140.81.Morphology.
11. Etminan N, Rinkel GJ. Unruptured intracranial aneurysms: development, rupture and preventive management. Nat Rev Neurol. 2016;12:699. http://dx.doi.org/10.1038/nrneurol.2016.150.
12. Fan J, Wang Y, Liu J, et al. Morphological-Hemodynamic Characteristics of Intracranial Bifurcation Mirror Aneurysms. World Neurosurg. 2015;84(1):114-120.e2. doi:10.1016/j.wneu.2015.02.038.
13. Ford MD, Hoi Y, Piccinelli M, Antiga L, Steinman DA. An objective approach to digital removal of saccular aneurysms: Technique and applications. Br J Radiol. 2009;82(SPEC. ISSUE 1):55-61. doi:10.1259/bjr/67593727.
14. Gabriel RA, Kim H, Sidney S, et al. Ten-year detection rate of brain arteriovenous malformations in a large, multiethnic, defined population. Stroke. 2010;41(1):21-26. doi:10.1161/STROKEAHA.109.566018.
15. de Gast AN, Soepboer A, Sluzewski M, van Rooij WJ, Beute GN. How long does it take to coil an intracranial aneurysm? Neuroradiology. 2008;50(1):53-56. doi:10.1007/s00234-007-0301-6.
16. Greving JP, Wermer MJH, Brown RD, et al. Development of the PHASES score for prediction of risk of rupture of intracranial aneurysms: a pooled analysis of six prospective cohort studies. Lancet Neurol. 2014;13(1):59-66. doi:10.1016/S1474-4422(13)70263-1.
17. Guha D, Ibrahim GM, Kertzer JD, Macdonald RL. National socioeconomic indicators are associated with outcomes after aneurysmal subarachnoid hemorrhage: a hierarchical mixed-effects analysis. J Neurosurg. 2014;121(5):1039-1047. doi:10.3171/2014.7.JNS132141.

18. Hoffman H, Toshkezi G, Swarnkar A, Gould G, Chin LS, Krishnamurthy S. A retrospective comparison of sac and lobe morphology between ruptured and unruptured intracranial aneurysms. J Clin Neurosci. 2018;60:88-92. doi:10.1016/j.jocn.2018.09.025.
19. Huang ZQ, Meng ZH, Hou ZJ, et al. Geometric parameter analysis of ruptured and Unruptured aneurysms in patients with symmetric bilateral intracranial aneurysms: A Multicenter CT angiography study. Am J Neuroradiol. 2016;37(8):1413-1417. doi:10.3174/ajnr.A4764.
20. Jiang H, Shen J, Weng Y-X, et al. Morphology Parameters for Mirror Posterior Communicating Artery Aneurysm Rupture Risk Assessment. Neurol Med Chir (Tokyo). 2015;55(6):498-504. doi:10.2176/nmc.oa.2014-0390.
21. Jing L, Fan J, Wang Y, et al. Morphologic and Hemodynamic Analysis in the Patients with Multiple Intracranial Aneurysms: Ruptured versus Unruptured. PLoS One. 2015;10(7):e0132494. doi:10.1371/journal.pone.0132494.
22. Lecler A, Raymond J, Rodriguez-régent C, Shareef F Al, Trystram D. Intracranial Aneurysms : Recurrences More than 10 Years after Endovascular Treatment — A Prospective Cohort Study , Systematic. Radiology. 2015;277(1):173-180.
23. Loewenstein JE, Gayle SC, Duffis EJ, Prestigiacomo CJ, Gandhi CD. The natural history and treatment options for unruptured intracranial aneurysms. Int J Vasc Med. 2012;2012. doi:10.1155/2012/898052.
24. Meng H, Tutino VM, Xiang J, Siddiqui A. High WSS or Low WSS? Complex interactions of hemodynamics with intracranial aneurysm initiation, growth, and rupture: Toward a unifying hypothesis. Am J Neuroradiol. 2014;35(7):1254-1262. doi:10.3174/ajnr.A3558.
25. Molyneux AJ, Birks J, Clarke A, Sneade M, Kerr RSC. The durability of endovascular coiling versus neurosurgical clipping of ruptured cerebral aneurysms: 18 year follow-up of the UK cohort of the International Subarachnoid Aneurysm Trial (ISAT). Lancet. 2015;385(9969):691-697. doi:10.1016/S0140-6736(14)60975-2.
26. Piccinelli M, Steinman D a, Hoi Y, Tong F, Veneziani A, Antiga L. Automatic neck plane detection and 3D geometric characterization of aneurysmal sacs. Ann Biomed Eng. 2012;40(10):2188-2211. doi:10.1007/s10439-012-0577-5.
27. Raghavan ML, Ma B, Harbaugh RE. Quantified aneurysm shape and rupture risk. J Neurosurg. 2005;102(2):355-362. doi:10.3171/jns.2005.102.2.0355.
28. Ruan C, Long H, Sun H, et al. Endovascular coiling vs. surgical clipping for unruptured intracranial aneurysm: A meta-analysis. Br J Neurosurg. 2015;29(4):485-492. doi:10.3109/02688697.2015.1023771.
29. Schneiders JJ, Marquering HA, Antiga L, Van Den Berg R, Van Bavel E, Majoie CB. Intracranial aneurysm neck size overestimation with 3D rotational angiography: The impact on intra-aneurysmal hemodynamics simulated with computational fluid dynamics. Am J Neuroradiol. 2013;34(1):121-128. doi:10.3174/ajnr.A3179.
30. Schneiders JJ, Marquering HA, Van Den Berg R, et al. Rupture-associated changes of cerebral aneurysm geometry: High-resolution 3D imaging before and after rupture. Am J Neuroradiol. 2014;35(7):1358-1362. doi:10.3174/ajnr.A3866.
31. Schnell S, Ansari SA, Vakil P, et al. Three-dimensional hemodynamics in intracranial aneurysms: influence of size and morphology. J Magn Reson imaging. 2014;39(1):120-131. doi:10.1002/jmri.24110.
32. Taubin G. Curve and surface smoothing without shrinkage. Proc IEEE Int Conf Comput Vis.:852-857. doi:10.1109/ICCV.1995.466848.
33. Thompson BG, Brown RD, Amin-Hanjani S, et al. Guidelines for the Management of Patients With Unruptured Intracranial Aneurysms: A Guideline for Healthcare Professionals From the American Heart Association/American Stroke Association. Vol 46.; 2015. doi:10.1161/STR.0000000000000070.
34. Tremmel M, Dhar S, Levy EI, Mocco J, Meng H. Influence of intracranial aneurysm-to-parent vessel size ratio on hemodynamics and implication for rupture: results from a virtual

experimental study. Neurosurgery. 2009;64(4):622-30; discussion 630-1. doi:10.1227/01.NEU.0000341529.11231.69.
35. Villablanca JP, Duckwiler GR, Jahan R, et al. Natural history of asymptomatic unruptured cerebral aneurysms evaluated at CT angiography: growth and rupture incidence and correlation with epidemiologic risk factors. Radiology. 2013;269(1):258-265. doi:10.1148/radiol.13121188.
36. Wilson S, Woo HH, Dlouhy BJ, et al. Accuracy of detecting enlargement of aneurysms using different MRI modalities and measurement protocols. J Neurosurg. 2018;130(February):1-7. doi:10.3171/2017.9.jns171811.
37. Xiang J, Natarajan SK, Tremmel M, et al. Hemodynamic-morphologic discriminants for intracranial aneurysm rupture. Stroke. 2011; 42(1):144-152. doi:10.1161/STROKEAHA.110.592923.
38. Xu J, Yu Y, Wu X, et al. Morphological and hemodynamic analysis of mirror posterior communicating artery aneurysms. PLoS One. 2013; 8(1):e55413. doi:10.1371/journal.pone.0055413.